

Observation of focused shock waves used for orthopaedic therapy

Conference Paper

Author(s):

Chaves, H.; Menne, A.

Publication date:

2018-10-05

Permanent link:

<https://doi.org/10.3929/ethz-b-000279163>

Rights / license:

[In Copyright - Non-Commercial Use Permitted](#)



OBSERVATION OF FOCUSED SHOCK WAVES USED FOR ORTHOPAEDIC THERAPY

H. Chaves^{1,c}, A. Menne²

¹Institute for Mechanics and Fluid Dynamics, Technical University of Freiberg, 09599 Freiberg, Germany

²E.M.S. Electro Medical Systems S.A., 1260 Nyon, Switzerland

^cCorresponding author: Tel.: +493731393318; Fax: +493731393455; Email: Humberto.Chaves@imfd.tu-freiberg.de

KEYWORDS:

Main subjects: wave propagation, flow visualization, wave focusing

Fluid: high speed flows, cavitation

Visualization method(s): shadowgraphy, high speed, phase locked imaging

ABSTRACT: *The waves produced by a submerged focusing shock wave generator, Piezoclast, EMS, Switzerland are observed using a pulsed LED (100ns) and backlit set-up. The trigger source is inductively coupled with the high voltage pulse driving the piezoelectric generator. This allows a high repeatability and a temporal resolution of phase locked full size images at an equivalent framing rate of 5 million frames per second. The waves propagate in a very reproducible manner with the sound speed of the liquid, water. Behind the forerunning shock wave an expansion wave reduces the pressure to a level below the vapour pressure creating a localized but stochastic cloud of cavitation bubbles. The interaction of waves with the bubble field shows a periodic fluctuation of the bubble sizes in the later stages of the process. There is a strong coupling through the pressure field in the liquid between the bubbles of the cloud. The shocks caused by the collapse of singular bubbles have time scales in the order of 0.5 μ s.*

1 Introduction

In the last twenty years there has been a rapid development of a field in orthopaedics named extracorporeal shock wave therapy for the treatment of for example chronic plantar fasciopathy or calcifying tendonitis of the shoulder, [1]. The background of this type of therapy is the application of shock waves, either focused or radially expanding, localized at the areas of a painful ailment. The effect of the shock waves on tissue has not yet completely understood [2], but both the direct effect of shock energy on the tissue as well as the indirect effect of cavitation bubbles produced by the relief wave after the positive pressure rise of the shock seem to have a biological effect. Focused shock waves break renal calculi in lithotripters. Due to the very high energy of these waves the cavitation bubbles formed after the shock cause lesions when they collapse, [3]. The purpose of the present work is to have a close look at the physical phenomena that occur when a wave focuses in water under laboratory conditions which allow a much better temporal as well as spatial resolution as could be achieved in vivo. This is viable since human tissue consists mainly of water.

2 Methods

2.1 Shadowgraphy and Schlieren

The observation of the shock waves bases on a shadowgraph and schlieren effect. The strong pressure gradients produced by the shock waves also have an effect on the liquid density and thus also on the refractive index of the liquid. For weak shock waves this effect cannot be detected. In the present case

however, not even a schlieren edge is necessary; the limited aperture of the lens is sufficient. What does need some effort is however the illumination of the images.

2.2 Pulsed incoherent image illumination

The waves propagate with a velocity comparable to the sound velocity in the liquid, i.e. 1500 m/s. For a field of view of 152 mm resolved with 1000 pixels the illumination can only last for 100 ns to avoid motion blur of the images. A pulsed laser can easily deliver pulses much shorter than this value, but a laser is coherent radiation and this would result in speckle in the images. Furthermore, the pulse to pulse fluctuation of lasers can be quite large. Here a light emitting diode (LED) pulsed for 100 ns with 10 amperes delivered the incoherent light pulse. The fluctuation from pulse to pulse in this case is smaller than the intensity resolution of the camera. As we will later on see, this is a very useful property of pulsed illumination with LEDs.

2.3 Phase locked image acquisition

To observe the propagation of the waves the temporal resolution should be in the order of the time interval the waves need to propagate (1500 m/s) across the image (0.152 m) divided by let's say 100 images. In the present case this corresponds to about 1 μ s interval between the images. There exist some high speed cameras that can resolve this with almost full frame resolution. The basic concept here was a different one. Provided the phenomena are reproducible and repeatable, one can make one image per realization of the experiment. The effective temporal resolution that depends on the trigger that has to be synchronous with the phenomena. The trigger uncertainty or jitter determines the resolution.

2.4 The wave generator

For these experiments a piezoelectric generator produces the shock waves, (Piezoclast, EMS, Switzerland). Multitudes of piezo ceramic crystals covering a concave metallic surface expand in response to a high voltage pulse to their electrodes. Precisely this high voltage pulse is the key to an appropriate trigger signal. A coil of ten loops around the hand piece of the piezoclast couples inductively and gives a voltage peak simultaneous to the deflection of the piezo ceramic crystals. This trigger signal has a temporal uncertainty smaller than 50 ns. It is captured with a LeCroy Waverunner oscilloscope and the trigger output of the oscilloscope is used to start a variable digital, quartz controlled delay. Various series of images were acquired with resolutions of 0.2 μ s and 1 μ s.

2.5 The optical set-up

The optical set-up consisted of a 5 mm LED whose light was collimated with a small aspheric lens of $f=18$ mm and made parallel with a Plexiglas lens of 300 mm diameter and 700 mm focal length. The parallel light beam then traversed the water tank in which the hand piece of the Piezoclast was partly submerged. On the other side of the water aquarium a second Plexiglas lens served as a field lens and together with a 75 mm objective imaged the field of view onto the chip of a PCO 1600 camera. Due to the high aperture collimation lens most of the light produced by the LED finally ends up on the chip of the camera. This is why it is possible to take images with a small LED.

2.6 Image post-processing

A further advantage of using a LED for illumination is the minimal pulse to pulse variation. This allows dividing the images pixelwise by a reference image taken before the experiment and then multiplying the result by 200. The action of this procedure is depicted on Figure 1. The optical set-up

uses large Plexiglas lenses that have some scratches and other imperfections, see the reference, the original and the original with noise reduction. Furthermore, the illumination is by no means homogeneous. All of these effects disappear on the divided (normalized) image. The images are now comparable with theoretical predictions since the effect of illumination intensity has been removed.

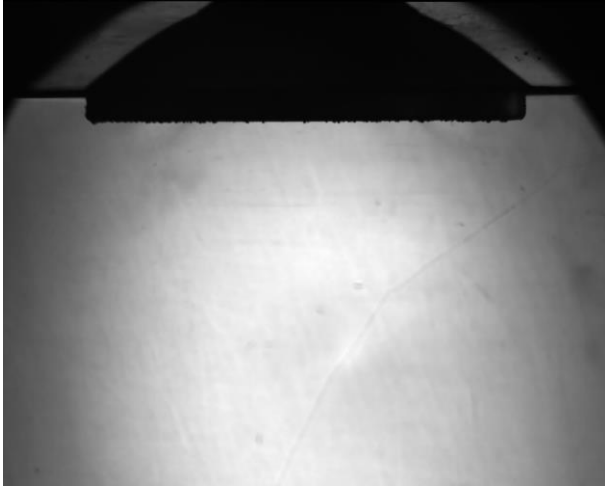


Fig. 1a. Reference image

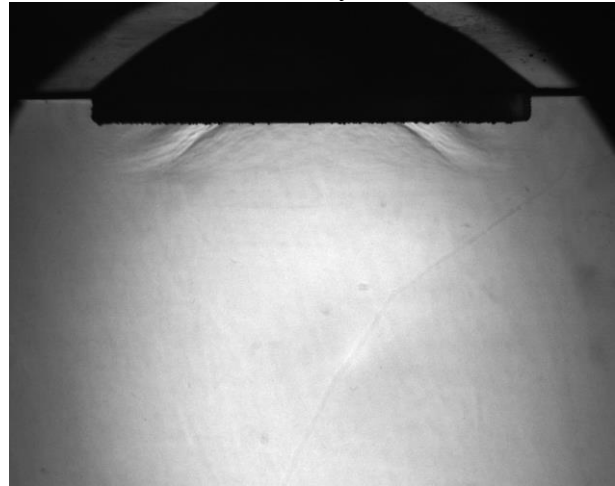


Fig. 1b. Original image

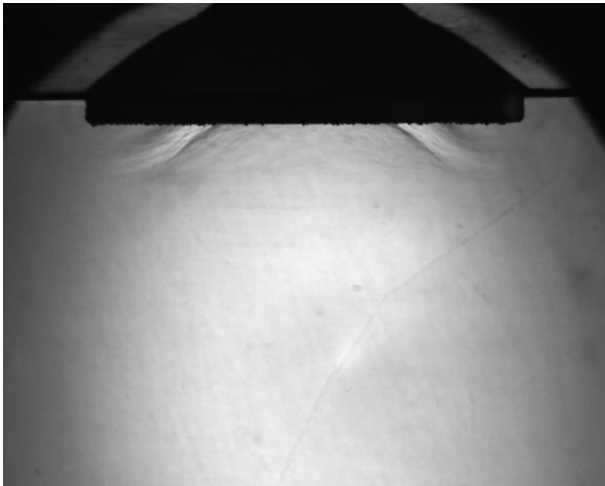


Fig. 1c. Noise reduction

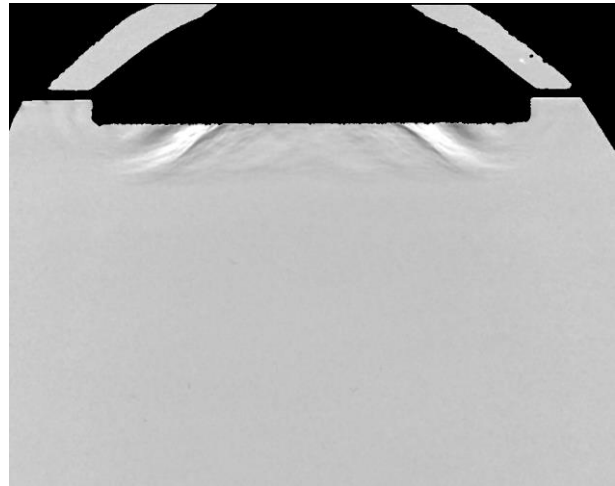


Fig. 1d. Result of the division by the reference

3 Results

Firstly, results will be shown taken from the image series with $1 \mu\text{s}$ temporal resolution, Figure 2. Of course, not all images can be shown here and a set of 8 images spanning a time of $60 \mu\text{s}$ were chosen to give an impression of the phenomena that occur during the experiment. The hand piece of the Piezoclast appears as a black dome at the top of the images in Figure 1. On Figure 2 the image of the handpiece has been cut away so that eight images can fit on one page. Its diameter is 11 cm. The structure of the waves is that of a thin black shock wave followed by an expansion wave lighter almost white area and a wide pressure rise to atmospheric pressure (gray). This is the structure of a so called N-wave. The shock wave is focused $34 \mu\text{s}$ after the piezo pulse at a distance of 41 mm from the rim of the hand piece. Above this region, where the expansion wave is focused cavitation bubbles appear together with secondary shocks coming from the collapse of singular bubbles. At later times the composite wave can be seen propagating radially outward from a source point more or less at the focus.

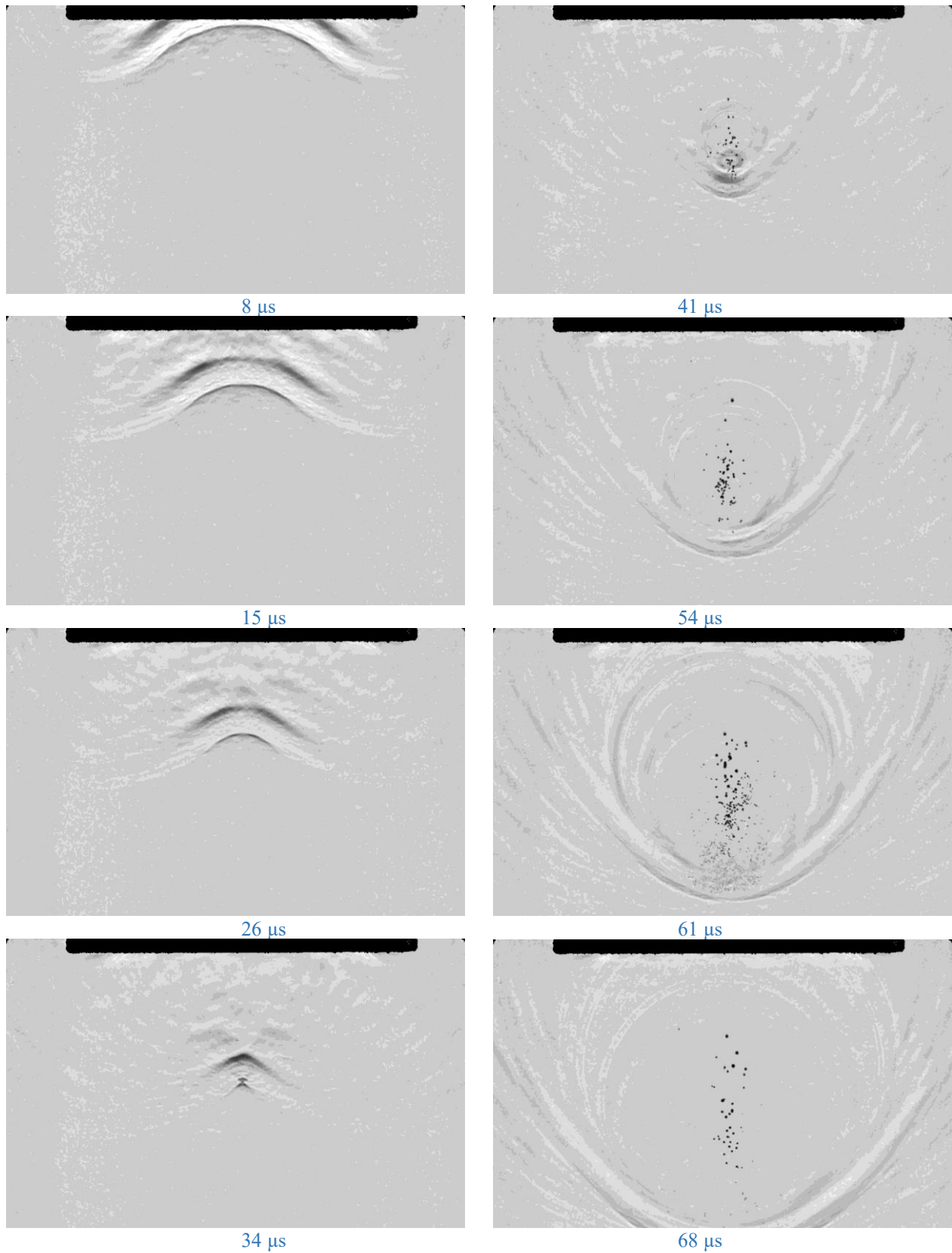


Figure 2. A series of images extracted from a sequence resolved with 1 μs , field of view 143.55 mm

These images are useful for the interpretation of the way this type of therapy functions and in particular where one can expect the highest local pressure and possible tissue damage due to cavitation collapse.

One could speculate that the wave could accelerate as it approaches the focal point because it is increasing in amplitude and if the wave strong enough non-linear effects would cause an increase in propagation velocity. Therefore, using images taken with $0.2 \mu\text{s}$ resolution the propagation of the central part of the wave was measured up to the focal point. Figure 3 shows the wave propagation diagram. The wave speed corresponds almost exactly to the sound speed in water and shows no sign of acceleration.

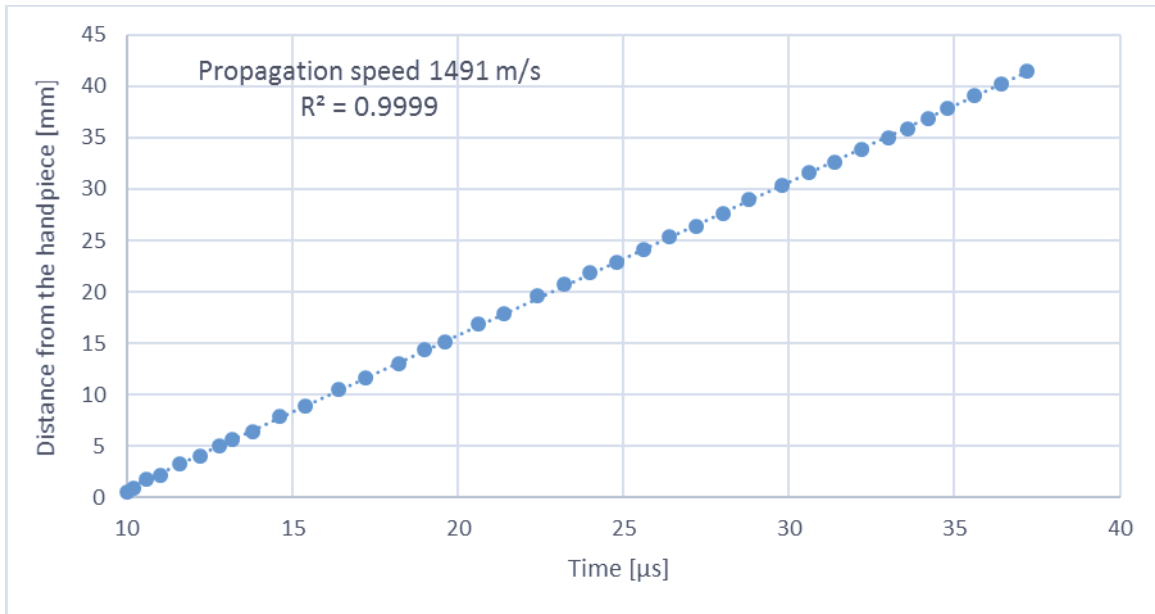


Figure 3. Wave propagation diagram

Figure 4 shows ten images of the cavitation bubbles created when the expansion wave focuses. The images have $0.2 \mu\text{s}$ temporal separation, but they are not from the same pulse. The shock wave propagates in a very deterministic manner, but the bubble fields are different for each new pulse, there is a stochastic element in the appearance of the bubbles. Most likely, it is the nucleation process which introduces this stochastic behavior. Although all images show bubbles they are not at exactly the same place but they are in an area behind the focus. One can see also circular waves of different sizes whose center is a bubble. Obviously, the bubbles are rebounding, i.e. after the collapse they do not disappear completely and grow again. The width of these waves on the images is about five pixel, which equals 0.76 mm in reality or corresponds to a duration of $0.5 \mu\text{s}$, which is longer than the pulse width of illumination, $0.1 \mu\text{s}$. They are therefore being resolved.

Later, see Figure 5 a periodic fluctuation in the order of $2 \mu\text{s}$ of the bubble clouds was detected showing collective behavior in the size and position of the bubbles in the cloud. Apparently, the behavior of a bubble in a cloud of bubbles is dependent of the behavior of the other bubbles in the cloud.

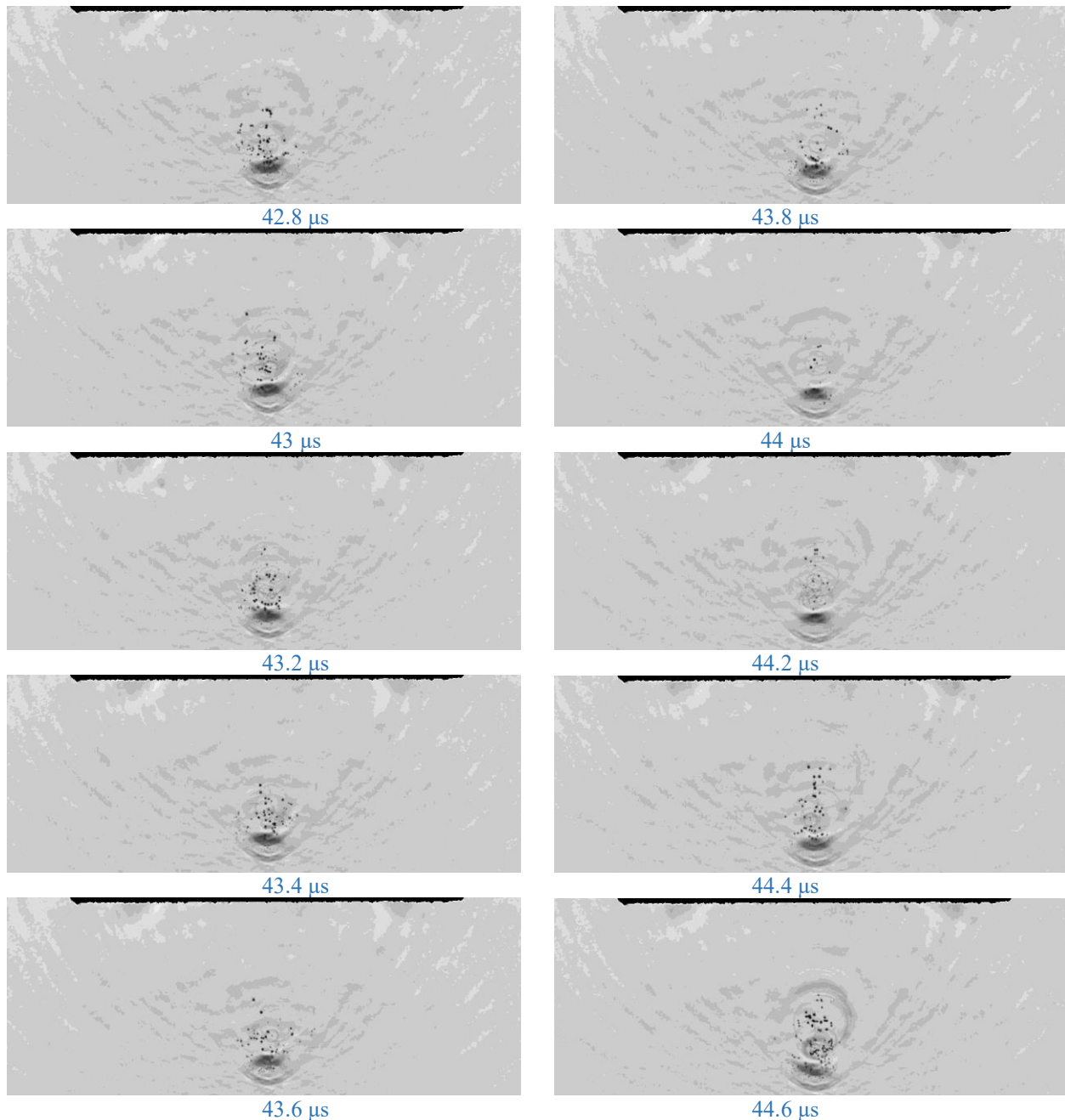


Figure 4. Collapsing cavitation bubbles and spherical shocks, sequence resolved with $0.2 \mu\text{s}$, field of view 143.55 mm

4 Conclusions

Although the propagation of shock waves is a very fast process, provided an appropriate trigger signal can be found a very high temporal resolution is achieved for repeatable and reproducible phenomena. In the present case, a temporal phase shift equivalent to 5 million frames per second was used to observe collective behavior of cavitation bubbles. Although the process entails some stochastic elements, an average bubble behavior can be observed. The shock waves themselves are very reproducible and deterministic phenomena.

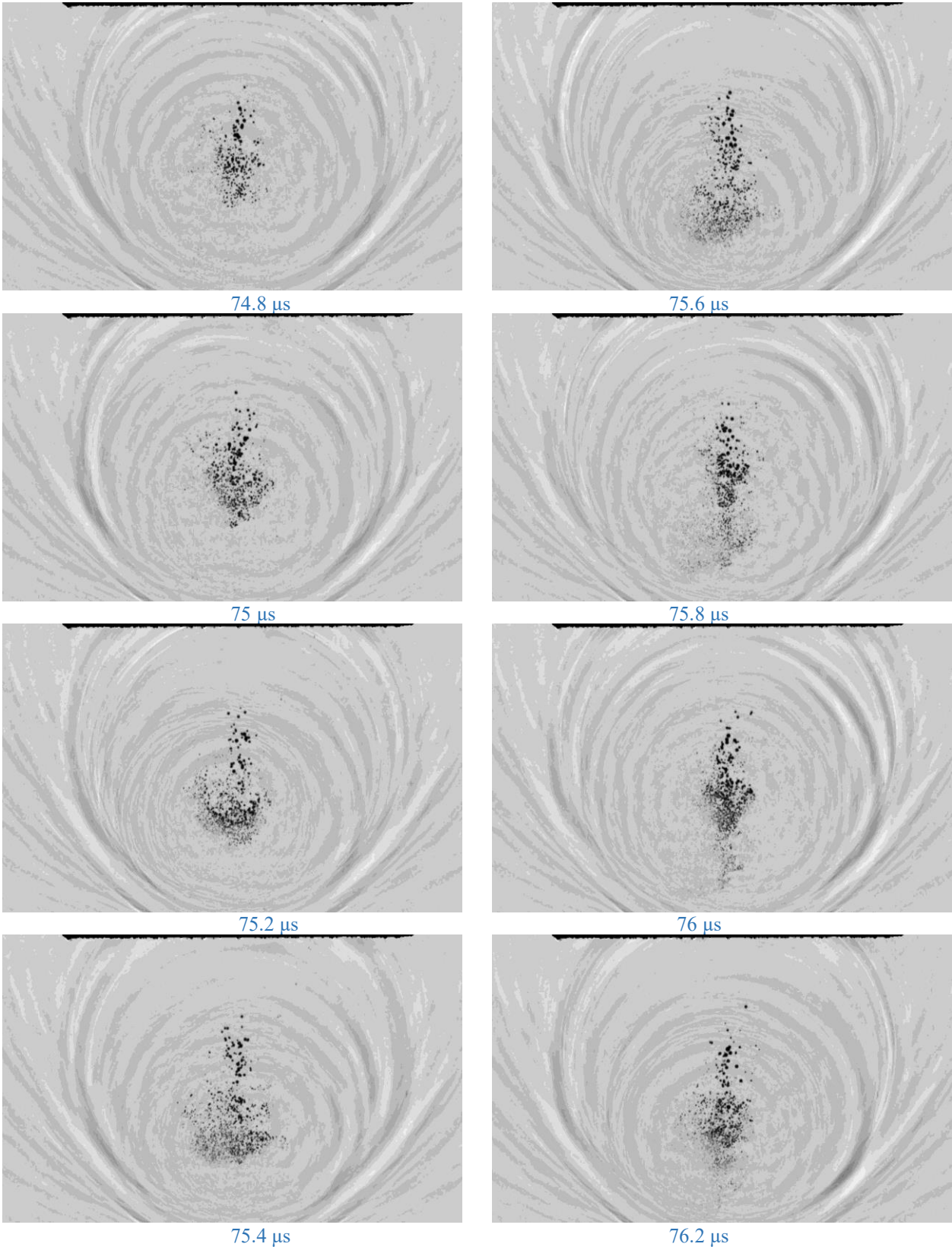


Figure 5. Collective behavior of a cavitation bubble cloud , field of view 143.55 mm

References

- [1] Schmitz et al.. Treatment of chronic plantar fasciopathy with extracorporeal shock waves (review). *Journal of Orthopaedic Surgery and Research*, 8:31, 2013.
- [2] Ioppolo, F., Rompe, J.D., Furla, J.P., Cacchio, A.. Clinical application of shock wave therapy (SWT) in musculoskeletal disorders(Review), *European Journal of Physical and Rehabilitation Medicine*, Vol. 50, No. 2, pp 217-230, 2014.
- [3] Yufeng Zhou. Reduction of Bubble Cavitation by Modifying the Diffraction Wave from a Lithotripter Aperture, *Journal of Endourology*, Vol.26, No. 8, pp 1075-1084, 2012.